Supporting Information for

# Membrane-Mediated Transport in Non-Equilibrium Hybrid Protocell Based on Coacervate Droplets and Surfactant

Haojing Chang, Hairong Jing, Yudan Yin, Qiufen Zhang, and Dehai Liang*

## Materials and Methods

**Materials.** A 21 nt single-stranded oligodeoxynucleotide (ss-oligo, 5′-CTTACGCTGAGTACTTCGATT-3′, $M_W$ = 6387 g/mol) with and without Cy5 fluorescence labelled at the 5'-terminus were purchased from Invitrogen. Poly-L-lysine (PLL, $M_W$ = 30 kDa~70 kDa), FITC-tagged PLL ($M_W$ = 30 kDa~70 kDa), DDAB, calcein, Rhodamine 6G, FITC-tagged dextran ($M_W = 4\times10^3$ g/mol) and horseradish peroxidase (HRP) were all purchased from Sigma-Aldrich (St. Louis, MI, USA). Polyvinylpyrrolidone ($M_W$: $3\times10^4$ g/mol) was purchased from Sinopharm Chemical Reagent Co., Ltd. All the materials were directly used without further purification. All the chemicals were dissolved in 4-Morpholine Ethane Sulfonic Acid (MES) buffer (20 mM, pH 6) to desired concentrations. Milli-Q water (18.2 MΩ·cm) was used throughout the experiments.

**Coacervate micro-droplets preparation.** The coacervate micro-droplets were prepared by mixing ss-oligo and PLL at predefined concentrations in a microfluidic channel (80 μm width × 25 μm depth). The channel was rinsed in sequence by 1.0 M NaCl, 1.0 M NaOH, 1.0 M HCl, Milli-Q water, and 1.0 % (w/w) MES-buffered polyvinylpyrrolidone, each for 10 min before use. The flow of ss-oligo and PLL in the channel was driven by gravity. The flow rate was determined by height of the solution in the well. At the same flow rate, the +/- charge ratio of the coacervate micro-droplets was controlled by the concentrations of ss-oligo and PLL before mixing. For the +/- =1.0, the concentration pair of ss-oligo/PLL was 1.5/1.0 mg $ml^{-1}$. After 2 min, the residual aqueous ss-oligo and PLL in the channel were replaced by 1.0 mM DDAB (above CMC) or 1.0 mM DDAB containing 1% BODIPY 558/568 $C_{12}$ (5.7 μM) to achieve coating. MES buffer was used to prepare uncoated coacervate micro-droplet as a control. After coated for 2 min, DDAB was replaced by MES buffer, and an electric field is applied to excite the micro-droplet.

**Transport experiments under applied electric field.** Calcein (20 mM), and Rhodamine 6G (8.9 mM) were used as the model micromolecules, whereas FITC-Dextran (1mg/ml), rhodamine isothiocyanate (RITC)-HRP (1mg/ml), Cy5-oligo (0.0157mg/ml), FITC-PLL (0.02mg/ml) were representing polysaccharide, enzyme and polyelectrolyte, respectively. These dyes or dye-labelled molecules with known concentration were introduced, separately, to the environment of the coacervate micro-droplet with or without DDAB coating. Images were taken 2 min after incubation. An electric field is employed to the system. The changes in droplet morphology, organization, and dynamics were recorded by a Laser Scanning Confocal Microscope (LSCM, A1R-si, Nikon, Japan). Calcein, Rhodamine 6G, RITC-, FITC- and Cy5- were excited at 494, 526, 543, 488, and 628 nm, respectively. The corresponding emissions were 517, 555, 580, 515 or 700 nm.

**Laser light scattering and zeta potential measurements.** The interaction between DDAB and PLL/ss-oligo complex whose concentrations were two orders lower than those used for coacervate droplet was studied by laser light scattering (LLS) and zeta potential analysis. PLL solutions (1.0 ml) were added into ss-oligo solutions (1.0 ml) dropwise in the cuvette to form complex with known charge ratios. The complex was vortexed for 10 s before adding 10 μl DDAB at 1.0 mg $ml^{-1}$. The one adding 10 μl buffer was used as a control. The samples stayed for 30 min before the measurement by LLS and zeta potential measurements.

LLS was conducted on a commercialized spectrometer (Brookhaven Inc., Holtsville, NY) over a scattering angular range of 20°−120°. A solid-state laser polarized vertically operating at 633 nm (Research Electro Optics, Inc. Colorado, USA) was used as the light source. A BI-TurboCo Digital Correlator (Brookhaven Instruments Corp.) was used for data analysis. In static light scattering (SLS), the angle was dependence of the excess scattered intensity, $I_{ex}=I_s-I_0$, where $I_s$ and $I_0$ represent the light intensity of the solution and solvent, respectively. In dynamic light scattering (DLS), the intensity−intensity time correlation function $G^{(2)}(\tau)$ in the self-beating mode was measured according to

$$G^{(2)}(\tau) = A\left[1 + \beta|g^{(1)}(\tau)|^2\right] \quad (1)$$

Where A is A is the measured baseline value, β is the coherence factor, τ is the delay time, and $g^{(1)}(\tau)$ is the normalized first-order electric field time correlation function. $g^{(1)}(\tau)$ is related to the line width distribution $G(\Gamma)$ by

$$g^{(1)}(\tau) = \int_0^\infty G(\Gamma)e^{-\Gamma\tau}d\Gamma \quad (2)$$

By using a Laplace inversion program, CONTIN, the normalized distribution function of the characteristic line width $G(\Gamma)$ was acquired. The average line width, $\bar{\Gamma}$, was calculated according to $\bar{\Gamma} = \int \Gamma G(\Gamma)d\Gamma$. $\bar{\Gamma}$ is a function of both C and q, which can be expressed as

$$\Gamma/q^2 = D(1 + k_d C)\left[1 + f(R_g q)^2\right] \quad (3)$$

with D, $k_d$, f being the translational diffusive coefficient, the diffusion second virial coefficient, and a dimensionless constant, respectively. D can be further transformed to the hydrodynamic radius Rh by using the Stokes-Einstein equation:

$$D = k_B T/6\pi\eta R_h \quad (4)$$

where $k_B$, T, η are the Boltzmann constant, the absolute temperature, and the viscosity of the solvent, respectively.

For LLS measurements, PLL and ss-oligo solutions were filtered, separately, through a 0.40 μm filter (Sartorius stedim Biotech, Goettingen, Germany) into a dust-free vial.

Zeta potential of the complex particles were evaluated at room temperature using a zeta potential analyzer (Zeta PALS, Brookhaven Instruments, Holtsville, NY). Zeta potential measurements were done with PLL/ss-oligo coacervate droplets prepared at the charge ratio of 1, with/without the presence of DDAB. Besides lower concentration, higher concentration that conducted in the microfluidic channel was also measured. Then samples were injected into a disposable zeta cuvette and the experiment was run using BIC PALS zeta potential analyzer software for data collection and processing.

**Small Angle X-ray scattering.** Small angle X-ray scattering experiments were undertaken on an Xenocs Ganesha using Cu Kα radiation as the X-ray source. The scattering patterns were recorded on an imaging-plate with the q (= 4π sin θ / λ, where λ is the wavelength of 0.1542 nm and 2θ is the scattering angle, respectively) value ranged from 0.06 to 29 $nm^{-1}$. The samples of PLL/ss-oligo micro-droplets coated with/without DDAB were prepared by following the same procedure as described LLS experiments, and loaded into a special glass capillary tubes (1.5 mm in diameter, Hilgenberg GmnH, Germany) for X-ray measurement. MES buffer at 20 μM and DDAB at 1mM were used as the control.

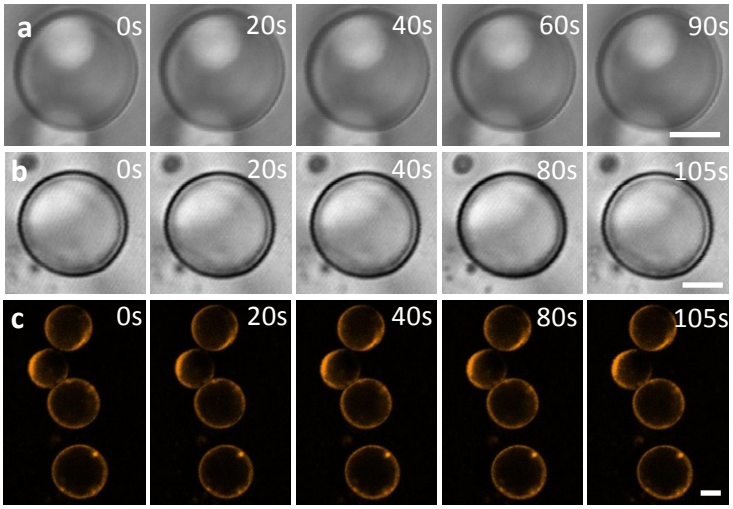


**Figure S1.** Time series of optical microscope images showing the behavior of a PLL/ss-oligo coacervate droplet at +/- =1 (a) without and (b) with 1.0 mM DDAB. The droplet is confined within a microfluidic channel and subjected to an electric field of 10 V $cm^{-1}$. Panel c shows the distribution of DDAB with BODIPY 558/568 $C_{12}$ as the probe. Scale bar, 5μm.

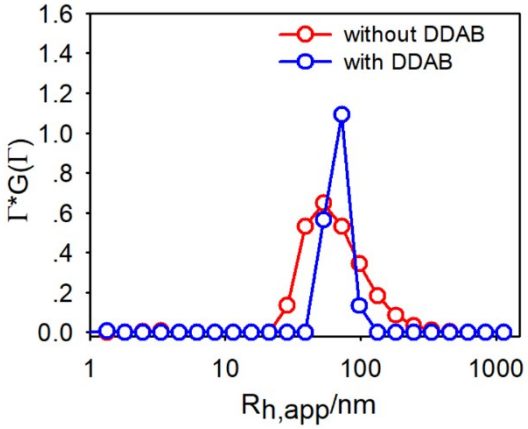

**Figure S2.** Size distribution of PLL/ss-oligo complex with or without DDAB at 30°.

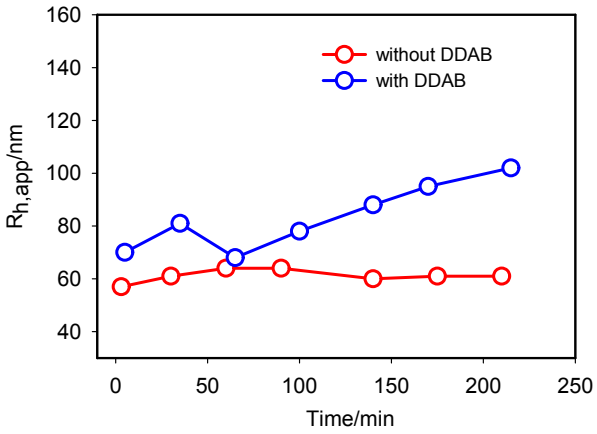


**Figure S3.** Time dependence of the hydrodynamic radius of PLL/ss-oligo complexes measured at 30°.

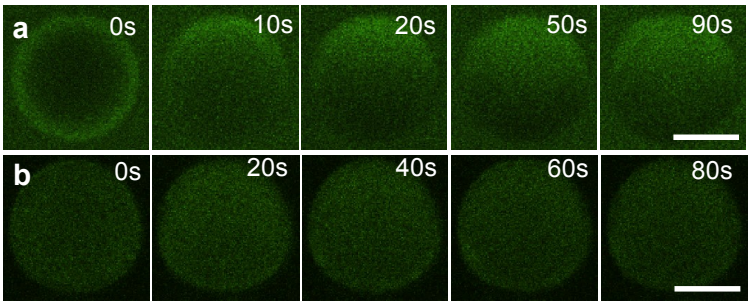


**Figure S4.** Fluorescence microscope images of calcein sequestration into PLL/ss-oligo coacervate micro-droplets at +/- =1 (a) without and (b) with DDAB in a microfluidic channel at an applied electric field of 10 V $cm^{-1}$. Scale bar, 5μm.

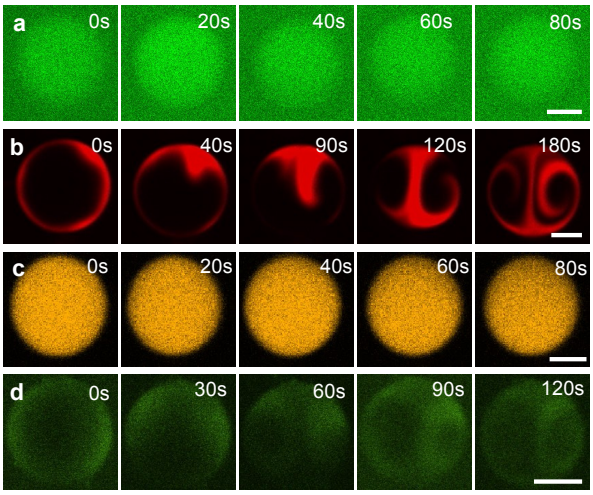

**Figure S5**. Time series of fluorescence microscope images showing the sequestration of (a) dextran, (b) ss-oligo, (c) Rho 6G, and (d) PLL into PLL/ss-oligo coacervate micro-droplets at +/- =1 at 10 V cm-1. No DDAB is present.

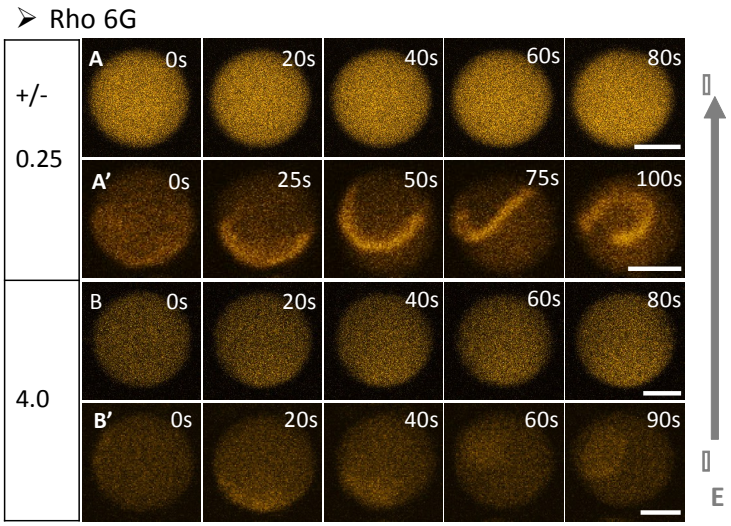


**Figure S6.** Time series of fluorescence microscope images showing the sequestration of Rho 6G into PLL/ss-oligo coacervate micro-droplet without (A)and with (A') DDAB at +/- =1 at 10 V $cm^{-1}$. The charge ratios of droplet are 0.25 and 4.0, separately.

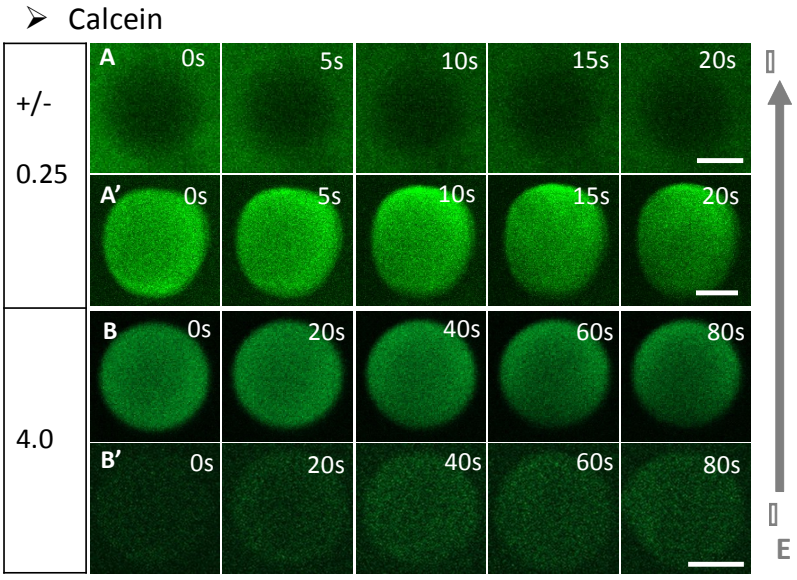


**Figure S7.** Time series of fluorescence microscope images showing the sequestration of calcein into PLL/ss-oligo coacervate micro-droplet without (A)and with (A') DDAB at +/- =1 at 10 V $cm^{-1}$. The charge ratios of droplet are 0.25 and 4.0, separately.

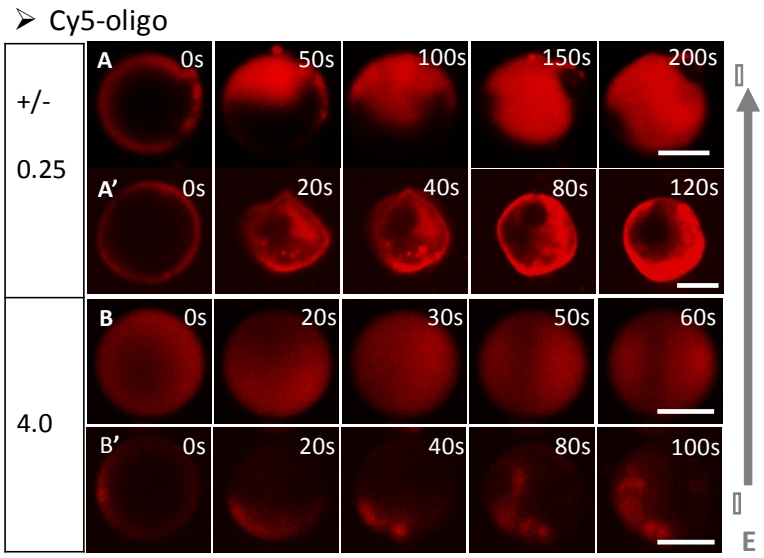


**Figure S8.** Time series of fluorescence microscope images showing the sequestration of Cy5-oligo into PLL/ss-oligo coacervate micro-droplet without (A)and with (A') DDAB at +/- =1 at 10 V $cm^{-1}$. The charge ratios of droplet are 0.25 and 4.0, separately.

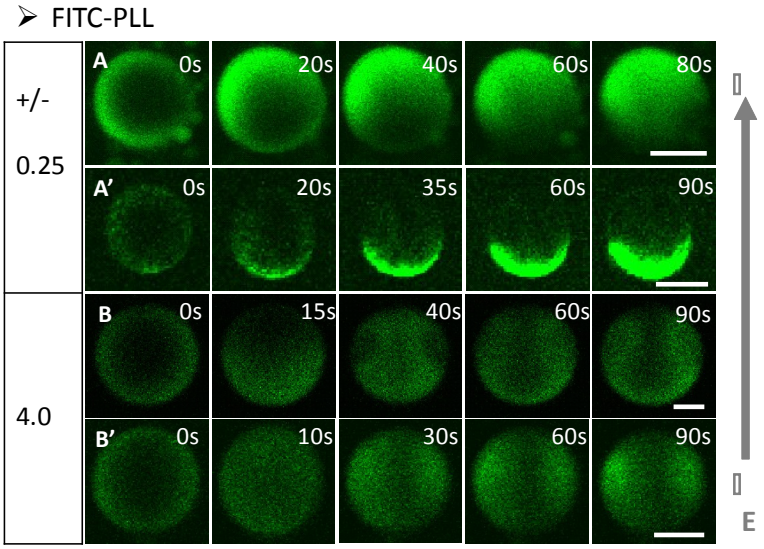


**Figure S9.** Time series of fluorescence microscope images showing the sequestration of FITC-PLL into PLL/ss-oligo coacervate micro-droplet without (A)and with (A') DDAB at +/- =1 at 10 V $cm^{-1}$. The charge ratios of droplet are 0.25 and 4.0, separately.